Chemical Composition and Crystal Structure of Graphite Fluoride

Yasushi Kita, Nobuatsu Watanabe,* and Yukio Fujii

Contribution from the Department of Industrial Chemistry, Faculty of Engineering, Kyoto University, Yoshida, Sakyo-ku, Kyoto 606, Japan. *Received July 11, 1978*

Abstract: The relation between the composition and crystal structure of graphite fluoride is studied. The formation of a new chemical compound, "polydicarbon monofluoride", represented by the formula $(C_2F)_n$, was confirmed under relatively mild direct fluorination of graphite. The composition of nonstoichiometric graphite fluoride prepared at temperatures less than 600 °C is not homogeneous but a mixture of $(CF)_n$ and $(C_2F)_n$. The fluorination of graphite first leads to the formation of $(CF)_n$ in the very thin film of surface followed by the formation of $(C_2F)_n$ and further fluorination again leads to the formation of $(CF)_n$. The ratio $(C_2F)_n/(CF)_n$, which is strongly dependent on the reaction temperature, decreases with increasing temperature. The composition of graphite fluoride with F/C ratio less than unity varies no longer even after the treatment at higher temperature in a fluorine atmosphere. The color of graphite fluoride does not depend on the composition but on the reaction and treatment temperature. The two-dimensional structure of $(C_2F)_n$ is regarded as a monoclinic system. The lattice constants are $a = 5.01$ Å, $b = 4.92$ Å, and $\gamma = 120.6°$. The stacking of the above layers is a turbostratic structure which consists of layers stacked randomly at the same distance of about 8.8 Å.

Graphite fluoride has been known since 1934, when Ruff and Bretschneider[1] had prepared a gray compound having a composition of $CF_{0.92}$. Rüdorff et al.[2-5] reported thereafter a series of studies on graphite fluoride in publications that appeared between 1947 and 1959. Their main results may be summarized as follows. The products with compositions ranging from $CF_{0.676}$ to $CF_{0.988}$ have been obtained by careful control of the reaction between graphite and gaseous fluorine around 410–550 °C. The fluorine-poor compounds are still black, and the color lightens with increasing fluorine content. The compound with the highest fluorine content is a pure white solid and its thin exfoliated layers are almost transparent. Hydrogen fluoride catalyzes the reaction of graphite with fluorine below 400 °C, where graphite is practically inert to fluorine. A fluorine–hydrogen fluoride mixture reacts with graphite at room temperature to give a compound having a composition of C_4F.

In spite of these pioneering studies, systematic studies on graphite fluoride have not been made for a long time because its utility had not been recognized at that time, and hence detailed studies have not been attempted on the reaction mechanism and physicochemical properties of the products.

Since 1961, Watanabe et al.[6-8] proposed that the anode effect in the production of elemental fluorine or aluminum by electrolysis is attributable to the formation of graphite fluoride film on the surface of a carbon electrode. This is due to a very low surface energy of graphite fluoride which served as a gaseous insulating film between electrode and bath. Since then a series of studies[9-24] on the reaction mechanism, the crystal structure, and the physicochemical properties of graphite fluoride have been carried out in order to develop the application of this compound to various practical fields. Also, fundamental studies of graphite fluoride have been reported by Margrave et al.[25-33] since 1965 and recently by others.[34-39]

Such unique physicochemical properties of graphite fluoride as low surface energy, solid lubricating characteristics, and oxidizing ability have been worthy of remark and applications in a wide variety of industrial fields have been proposed.[40-52] These characteristics strongly depend on the crystal structure of the products. However, the chemical composition of graphite fluoride obtained by direct fluorination of graphite at temperatures between 410 and 630 °C ranges from $CF_{0.68}$ to $CF_{1.12}$ and their interlayer spacings vary widely in the range from 8.9 to 5.76 Å.[1,2,11,14,16,27,31,32] There are $>CF_2$ and $-CF_3$ groups around the edges of the graphite fluoride layers.[15,32,38,39] Excess fluorine of that required to form a stoichiometric compound, $(CF)_n$, can be ascribed to this fact. On the other hand, $(CF_x)_n$ $(x < 1)$ has been regarded as a mixture of $(CF)_n$ and unreacted graphite or a homogeneous compound. However, no plausible explanation has been given for such large variations in the composition and interlayer spacing of graphite fluoride.

In this paper, experimental results with regard to the influences of reaction temperature, fluorine pressure, particle size of graphite, and graphitization degree of carbon on the composition and crystal structure of graphite fluoride are described. Based on the data obtained, the relation between the composition and crystal structure is discussed as follows: (1) chemical composition of graphite fluoride, (2) crystal structure and properties of graphite fluoride, (3) formation process of $(C_2F)_n$ and $(CF)_n$.

Experimental Section

I. Apparatus and Procedure for Fluorination of Graphite. Natural graphites from Madagascar ores with particle size of 200–250 (62–74 μm), 20–50 (279–840 μm), and more than 400 mesh (<37 μm) were used as the materials for fluorination.[53] The purity estimated from ash measurement was 99.5% and the impurities identified by atomic emission spectrochemical analysis were mainly various compounds of calcium, iron, and silicon.

The fluorination apparatus used was a thermobalance specially designed for fluorine gas.[21] About 25 mg of the graphite was spread uniformly on the sample pan, and then heated at 500 °C under vacuum (under less than 10^{-2} mmHg) for about 2 h to remove moisture. The fluorination has been carried out under a fluorine pressure of 200 mmHg in the temperature range between 375 and 640 °C. The fluorination under fluorine pressures of 100, 400, and 760 mmHg was also made in order to examine the pressure effect.

However, a fairly large amount of uniform sample is required for the measurements of NMR, heat of immersion, etc. In a conventional static reactor, the retardation in the diffusion of fluorine gas in the voids between particles during the progress of reaction causes the formation of an inhomogeneous sample. A rotary reactor shown in Figure 1 was therefore designed and constructed. The main parts of the apparatus were made of nickel because such parts as the reaction tube (2), the reaction vessel (1), and its supporting rod (3) were kept at high temperature during the reaction and other parts, which were at ambient temperature, were made of Polyflon (polytetrafluoroethylene, PTFE, Daikin Co.), Daiflon (polytrifluorochloroethylene, PTFCE, Daikin Co.), copper, and stainless steel. In view of the corrosive resistance to fluorine at high temperature, an evulsion pipe (950 mm in length, 60 mm o.d., and 50 mm i.d.) was used as the reaction tube. A leak-free seal around the reaction tube was achieved with a mechanical seal (11) which was filled with Daifloil (low molecular weight PTFCE, Daikin Co.). The mechanical seal is manufactured

0002-7863/79/1501-3832$01.00/0 © 1979 American Chemical Society

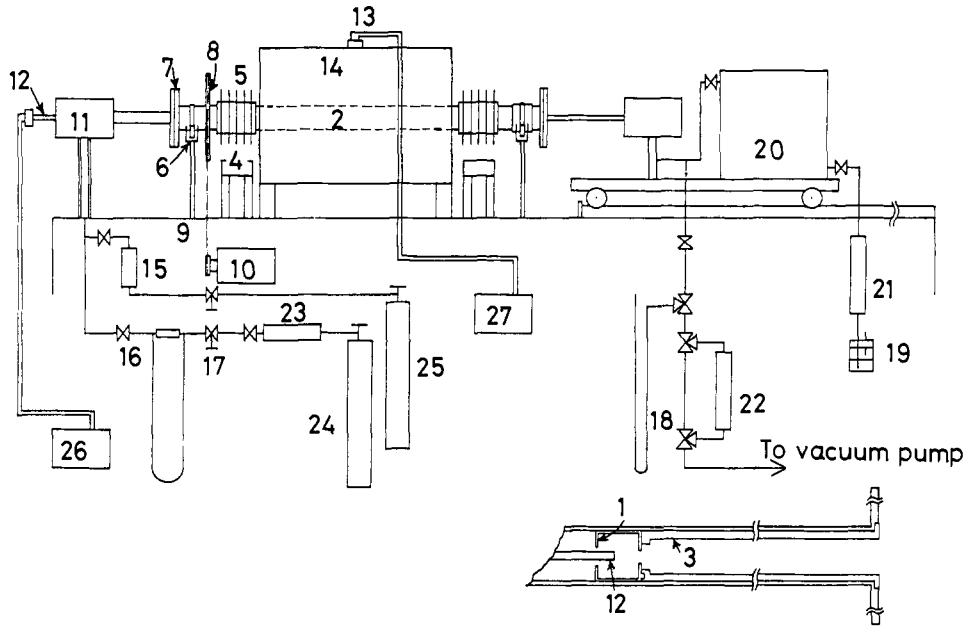

Figure 1. Schematic diagram of rotary reactor for fluorination: 1, reaction vessel; 2, reaction tube; 3, supporting rod of reaction vessel; 4, cooling fan; 5, fin made of aluminum; 6, support pole of reaction tube; 7, flange; 8, toothed wheel; 9, chain; 10, motor; 11, bearing (mechanical seal); 12, thermocouple for measurement; 13, thermocouple for controller; 14, furnace; 15, flow meter for argon; 16, orifice-type flow meter for fluorine; 17, regulator cock; 18, Hg manometer; 19, seal; 20-22, F_2 absorber (soda lime pellets); 23, HF absorber (NaF pellets heated to 100 °C); 24, F_2 gas; 25, Ar gas; 26, recorder; 27, temperature controller.

Table I. Fluorine Contents of Graphite Fluoride Prepared at Various Reaction Temperatures and Times

reaction temp, °C	formation time, h	fluorine, %
375	120	47.96
400	50	49.25
425	40	49.70
450	10	51.62
450	70[a]	51.45
475	5	53.13
475	50[a]	53.37
500	2.5	55.68
525	1.67	58.07
550	0.83	58.85
570	0.67	60.35[b]
570	120[a]	60.77[b]
600	0.33	61.30[b]

[a] The values are longer than actual formation time. [b] Determined by the method using sodium peroxide as a combustion aid.

by Torishima Pump Mfg. Co., Ltd. (LDU, 1107-5379-16ϕ, 20ϕ). The rotation number of the reaction tube was variable in the range between 2 and 50 rpm. The reaction temperature was measured by a chromel-alumel thermocouple (12) covered with nickel pipe, and controlled within ±1 °C. The difference in temperature of each part of the reaction vessel (50 mm in length and 45 mm i.d.) was within 5 °C. The fluorine gas used was typically of 98% purity. The HF present as a contaminant in the fluorine gas was fixed as $NaHF_2$ through NaF pellets heated at 100 °C (23). The flow rate of fluorine gas was measured with an orifice-type flow meter having an aperture of 0.1ϕ (16). The gage for measuring flow rate was made of PTFCE, and the liquid enclosed was low molecular weight PTFCE. In a mercury manometer (18), low molecular weight PTFCE was also used to separate mercury from fluorine gas.

Graphite (1-2 g) was placed in the reaction vessel and evacuated with a rotary pump to remove air and moisture. In the reaction at temperatures higher than 450 °C, the sample was first treated for 1 h at above 500 °C at a flow rate of 10 mL/min argon, and the furnace was set to the prescribed temperature. Then the reaction tube was rotated at 2 rpm and fluorine gas was flown to the reaction tube at a flow rate of 50 mL/min.

In the reaction at temperatures lower than 450 °C where no pyrolysis of graphite fluoride occurs, the sample was heat-treated at 500 °C under vacuum for 1 h, and the furnace was set to the prescribed temperature. Then fluorine gas was introduced at a rate of 50 mL/min to atmospheric pressure. During the reaction, the fluorine pressure was monitored by the manometer, and maintained almost at the atmospheric pressure, though the pressure drop was sometimes observed. The residual fluorine gas during the fluorination was removed by passing through the soda-lime tube (20) and (21). The exhaust of residual gas after a reaction was carried out through the soda-lime tube (22).

II. Microdetermination of Graphite Fluoride. The composition of graphite fluoride was determined by the fluorine content in the following manner.[54] Weighed samples of 1-3 mg were decomposed according to an oxygen flask combustion method,[55] and the fluorine was absorbed into water as hydrogen fluoride, but the fluorine content of the products prepared above 570 °C was determined by the method using sodium peroxide as a combustion aid. In the resulting hydrogen fluoride solution, fluorine was determined by an Orion Research Model 94-09A fluoride ion electrode.

Results and Discussion

I. Chemical Composition of Graphite Fluoride. Formation Time[56] of Graphite Fluoride at Various Temperatures. Table I shows the formation time for the graphite with particle size of 200-250 mesh. The formation times were evaluated by the weight change of sample. As shown with the number in parentheses, the F/C ratio did not change even after a long time. The formation time at 375 °C is 120 h, while at 600 °C it is only 20 min. Accordingly, the fluorination of graphite at each temperature has been carried out at least for more than the formation time.

As the reaction rate of graphite fluoride is proportional to the square root of fluorine pressure,[12] the formation time becomes longer with decreasing fluorine pressure. On the other hand, the reaction time becomes necessarily longer with increasing the particle size of the sample.

Effect of Reaction Temperature on the Composition of Graphite Fluoride. The dependence of the composition and color change of graphite fluoride on temperature is shown in Figure 2. The F/C ratio continuously increases from 0.58 at 375 °C to 1.03 at 640 °C with reaction temperature. With the increase in temperature, the color varies from black without a metallic luster at temperatures below 500 °C through gray

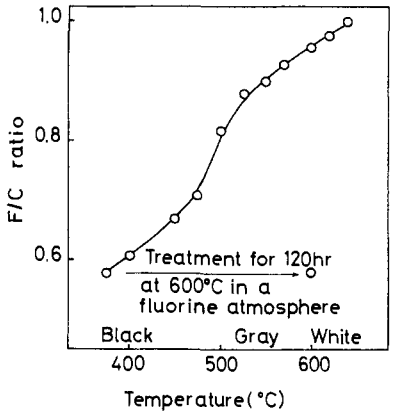

Figure 2. Dependence of F/C ratio of graphite fluoride on reaction temperature.

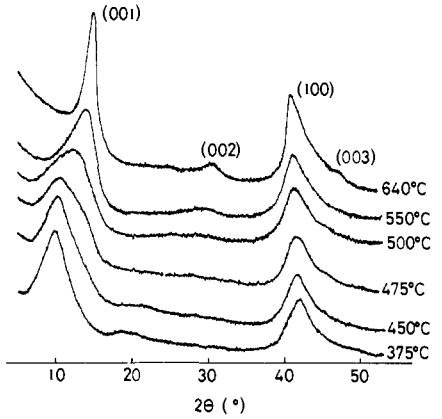

Figure 3. X-ray diffraction powder patterns of graphite fluoride prepared at various reaction temperatures.

to white or transparent at temperatures above 600 °C. It should be noted that the F/C ratio of the product prepared at 375 °C increased no longer even after the additional fluorination at 600 °C for 120 h (p_{F_2} = 200 mmHg).[57] However, its color varied from black to white. The product ($CF_{0.79}$) obtained by the fluorination at 500 °C also gave the same results. This means that the sample is completely fluorinated and, even if the F/C ratio of graphite fluoride is less than one, the product was not more fluorinated at a high temperature of 600 °C under fluorine atmosphere.

When the products prepared below 450 °C were placed in a vessel made of glass, the glass was tarnished some days after, the degree of which became larger with the decrease in the reaction temperature. This is due to the gradual release of the fluorine absorbed into the interlayer of graphite fluoride. In the case of these samples treated at 600 °C in a fluorine atmosphere, however, the glass was not tarnished.

Figure 3 shows the X-ray diffraction powder patterns of the products prepared at the same reaction conditions as in Figure 2. The position of the peak due to the (001) diffraction is shifted to higher angles and the half-width also changes according to the elevation of reaction temperature. On the other hand, the position of the peak due to the (100) diffraction is slightly shifted to lower angles. Although further fluorination of the product prepared at 375 °C was attempted, there was little variation in the diffraction pattern as well as the composition.

Figure 4 shows the variation of the interlayer spacing, $d_{(001)}$, and the half-width, $\beta_{(001)}$, of the (001) diffraction line of graphite fluoride with the reaction temperature.[58] The $d_{(001)}$ value of the product obtained by the reaction at 640 °C is 5.85 Å, while that of the product obtained at 375 °C is 9.0 Å. The

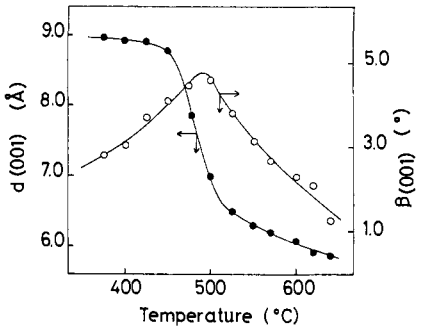

Figure 4. Variation of $d_{(001)}$ and $\beta_{(001)}$ of graphite fluoride with reaction temperature.

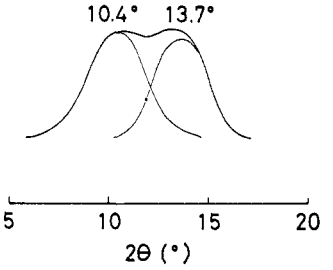

Figure 5. (001) profile corrected with Lorentz-polarization factor of graphite fluoride prepared at 425 °C.

interlayer spacings of the products obtained by the reaction at intermediate temperatures are between 5.85 and 9.0 Å. The $\beta_{(001)}$ value increases with the elevation of reaction temperature, shows a maximum at about 490 °C, and then decreases with further elevation of temperature. This suggests that the (001) diffraction patterns of the products fluorinated near 490 °C can be regarded as consisting of two components. For example, Figure 5 shows the (001) profile corrected with a Lorentz-polarization factor of the product prepared by the reaction of flaky graphite with fluorine at 425 °C for 163 h.[59] This diffraction pattern consists of a symmetrical diffraction line having a peak at 10.4° and that having a peak at 13.7°.

Based on the experimental evidence explained above, it is thought that graphite fluoride with an F/C ratio below one obtained by the reaction at temperatures of up to 600 °C consists of two different compounds each having interlayer spacings of about 6 and 9 Å. The former is polycarbon monofluoride, $(CF)_n$, which has been already reported as graphite fluoride. On the other hand, although the composition of the product prepared at 375 °C is $CF_{0.58}$, the composition of the compound having the interlayer spacing of about 9 Å would be C_2F. Minor differences in the composition between $CF_{0.58}$ and C_2F may be due to the facts that the sample contains $>CF_2$ and $-CF_3$ groups around the edges of the layers, that the fluorine absorbed into the interlayer, and that there exists a small amount of $(CF)_n$ in the sample. That is to say, the latter is polydicarbon monofluoride represented by the chemical formula $(C_2F)_n$. Thus the composition of nonstoichiometric graphite fluoride prepared at temperatures lower than 600 °C is not homogeneous compound but a mixture of $(CF)_n$ and $(C_2F)_n$. The fraction of two types of compounds is strongly dependent on the reaction temperature, and the fraction of $(C_2F)_n$ decreases according to the elevation of temperature; hence the compound with various apparent composition between $CF_{0.58}$ and $CF_{1.03}$ is obtained. Moreover, in order to obtain $(CF)_n$ alone, it is necessary to react at higher temperature, that is, 600–640 °C. On the other hand, it is possible to conclude that the products below 400 °C are mostly $(C_2F)_n$. Based on this proposition, we can clearly explain large variations in the composition and interlayer spacing of graphite fluoride reported to date.

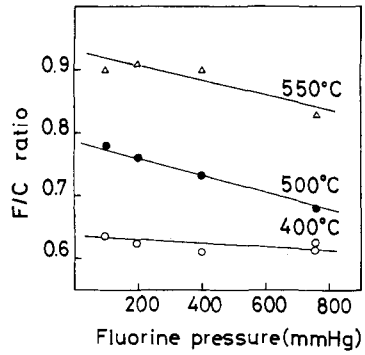

Figure 6. Dependence of F/C ratio of graphite fluoride on fluorine pressure.

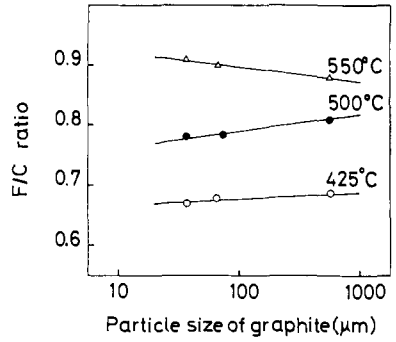

Figure 7. Dependence of F/C ratio of graphite fluoride on particle size of graphite.

Graphite fluoride is classified by the composition as follows: polycarbon monofluoride, $(CF)_n$; polydicarbon monofluoride, $(C_2F)_n$; polytetracarbon monofluoride, $(C_4F)_n$.[3,28] However, as C_4F is formed by the reaction of graphite with a fluorine–hydrogen fluoride mixture and hydrogen fluoride cannot be completely removed from the product, it can also be expressed as $C_n(HF)_xF_y (n \geq 4, 1 \geq x > y)$.[21]

Effect of Fluorine Pressure on the Composition of Graphite Fluoride. Figure 6 shows the dependence of the composition of graphite fluoride on fluorine pressure. At each temperature, the F/C ratio of graphite fluoride decreases with increasing fluorine pressure. These tendencies are remarkable in the product prepared at 500 °C. Generally, it can be said that the higher fluorine pressure is associated with the larger $(C_2F)_n$ content in the product.

Effect of Particle Size of Graphite on the Composition of Graphite Fluoride. Figure 7 shows the dependence of the composition of graphite fluoride on the particle size of graphite. At temperatures below 500 °C, the F/C ratio of graphite fluoride increases with increasing the particle size. Accordingly, the smaller the particle size, the more the $(C_2F)_n$ content of the product is. However, when the particle size decreases, the reaction rate of graphite fluoride becomes larger so that the elevation of reaction temperature and resulting decomposition of the products tend to occur at high temperature. Conversely, the fraction of $(CF)_n$ increases with decreasing the particle size at 550 °C.

Effect of Graphitization Degree of Carbon on the Composition of Graphite Fluoride. Watanabe et al.[14] have previously reported the variation of the fluorine content and interlayer spacing of graphite fluoride with the heat-treatment temperature of petroleum coke as shown in Figure 8. That is to say, the fluorine content of graphite fluoride decreases according to the elevation of heat-treatment temperature, and the interlayer spacing reaches a minimum at a temperature of 2000 °C. This can be understood by the view that, as in the case of graphite, the advancement of crystallization of petroleum coke

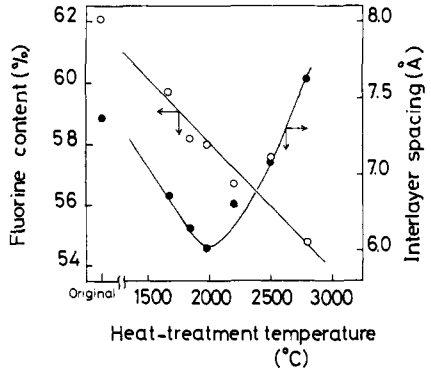

Figure 8. Variation of fluorine content and interlayer spacing of graphite fluoride with heat-treatment temperature of petroleum coke.

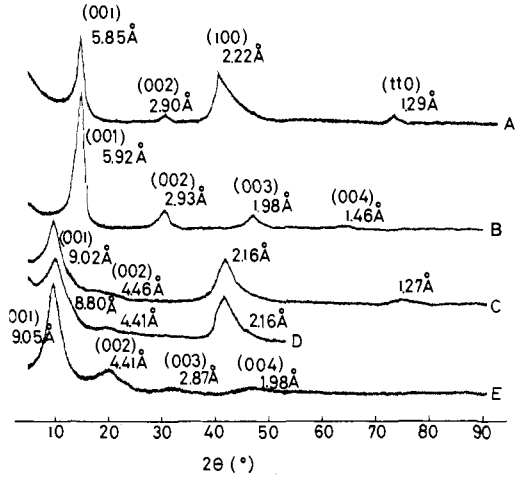

Figure 9. X-ray diffraction patterns of $(CF)_n$ and $(C_2F)_n$.

leads to preferential formation of $(C_2F)_n$. The large interlayer spacing of graphite fluoride prepared from the low crystalline petroleum coke results from the crystallinity of the original material.

II. Crystal Structure and Properties of Graphite Fluoride. In addition to polycarbon monofluoride, $(CF)_n$, denoted as graphite fluoride so far, the formation of a novel chemical compound, polydicarbon monofluoride, represented by $(C_2F)_n$, was confirmed in the reaction of fluorine with graphite under mild reaction conditions. The crystal structure and properties of $(CF)_n$ have already been reported by many investigators.[15-17,29,32,33,37,38] In the present section, the crystal structure and physicochemical properties of $(C_2F)_n$ are studied by means of X-ray and electron diffractometries, ESCA, IR, and many other experimental methods. The results are discussed in comparison with those of $(CF)_n$. The starting materials and the fluorination conditions of the graphite fluoride measured are given in Table II.

X-ray Diffraction Pattern. Figure 9 shows the X-ray diffraction patterns of $(CF)_n$ and $(C_2F)_n$. In a flaky sample, $(hk0)$ reflections are missing because of the orientation of the sample. From the diffraction lines of $(CF)_n$ in the figure, the interplanar spacings were calculated to be 5.85, 2.90, 2.22, and 1.29 Å from the pattern A, and 5.92, 2.93, 1.98, and 1.46 Å from the pattern B. The lattice constants, $a = b = 2.57$ Å, in a layered structure of $(CF)_n$ were obtained by the above data.

If a three-dimensional model was assumed for the structure $(CF)_n$, the three types of stacking designated as (AA...), (ABAB...), and (ABCABC...) could be considered as shown in Figure 10. As the surface energy of $(CF)_n$ is 38–47 ergs/

Table II. Starting Materials and Reaction Conditions of Graphite Fluoride

sample	starting material	reaction condition: temp, °C	reaction condition: fluorine pressure, mmHg	reaction condition: time, h
A	graphite (200–250 mesh)	640	200	36
B	graphite (20–50 mesh)	635	200	45
C	graphite (200–250 mesh)	370	760	132
D	sample (C) treated at 600 °C for 120 h in F_2 (200 mmHg)			
E	graphite (20–50 mesh)	375	760	180
F	graphite (20–50 mesh)	620	200	48
G	graphite (20–50 mesh)	375	200	120
H	sample (G) treated at 600 °C for 120 h in F_2 (200 mmHg)			
I	petroleum coke	400	200	4
J	graphite (200–250 mesh)	375	200	120
K	sample (J) treated at 600 °C for 120 h in F_2 (200 mmHg)			
L[a]	graphite (250–300 mesh)	375	760	179
M[a]	sample (L) treated at 600 °C for 24 h in F_2 (200 mmHg)			
N[a]	graphite (250–300 mesh)	620	50 mL/min (Ar, 10 mL/min)	24
O[a]	graphite (250–300 mesh)	354	760	144
P	sample (O) treated at 600 °C for 10 h in F_2 (200 mmHg)			
Q[a]	graphite (250–300 mesh)	488	50 mL/min (Ar, 10 mL/min)	18
R	graphite (200–250 mesh)	600	200	120

[a] Sample prepared by a rotary reactor.

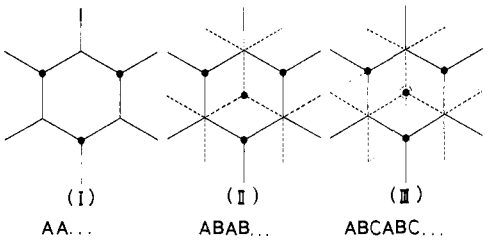

Figure 10. Stacking structure of $(CF)_n$: ▲, C–F bond up; ▽, C–F bond down; —, sequence A; - - - -, sequence B; ····, sequence C.

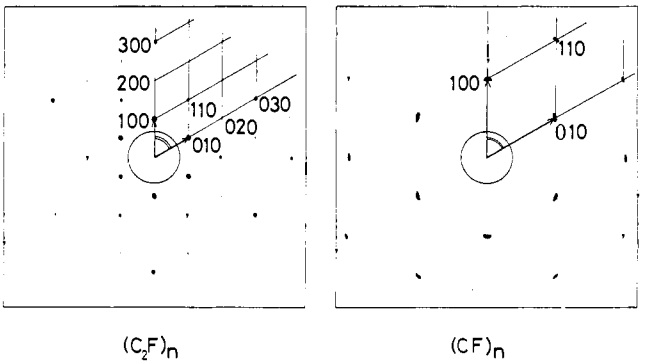

Figure 11. Reciprocal lattices for the basal plane of $(C_2F)_n$ and $(CF)_n$.

cm^2 [60] and is less than one-third of that of graphite, the interlayer binding energy of $(CF)_n$ may be very small. In addition, the difference in potential energy among the three types of stacking may be extremely small, and the layers are rearranged to each other so that $(CF)_n$ may have a turbostratic structure.[61] Actually, the diffraction patterns consist of (00*l*) and (*hk*0) reflections and an (*hk*0) diffraction line; for example, the (100) line rises very rapidly near the position of the maximum and then falls off slowly toward a larger angle.[62] Therefore, the Miller index of the crystal face cannot be accurately determined, and the (00*l*) diffraction, which shows the interlayer spacing of $(CF)_n$, is assumed to be the (001) diffraction, and the other diffraction lines are indexed as shown in Figure 9 in a similar manner as described previously.[16,33]

From the diffraction lines of $(C_2F)_n$, C and E in Figure 9, interplanar spacings of 9.02, 4.46, 2.16, and 1.27 Å and 9.05, 4.41, 2.87, and 1.98 Å were calculated, respectively. Indices for (00*l*) reflections of $(C_2F)_n$ were determined in a similar manner as those of $(CF)_n$. The (001) diffraction line in sample E has a peak at 9.76°, but the peak is shifted to at about 10° by a Lorentz-polarization factor. This interlayer spacing is 8.8 Å. The diffraction lines having a peak at 41.85 and 74.8° are due to the reflections of type (*hk*0) because they are missing in the diffraction pattern of the flaky sample.

When a low-crystallinity $(C_2F)_n$ prepared at 370 °C is heat-treated at 600 °C for 120 h in a fluorine atmosphere, it changes to high crystallinity so that the (001) diffraction line slightly shifts to higher angle.

Electron Diffraction Pattern. The symmetry of the lattice in a layered structure was evaluated by means of electron diffractometry. The sample was arranged in such a way that an electron beam incidence is perpendicular to the basal plane of the graphite fluoride crystal. Figure 11 shows the electron diffraction patterns of $(CF)_n$ and $(C_2F)_n$. The arrangement of two-dimensional lattice points of $(CF)_n$ shows a sixfold rotating symmetry, and the two-dimensional structure belongs to a hexagonal system.[16] That of $(C_2F)_n$ does not show a complete sixfold rotating symmetry but a twofold rotating symmetry as shown in the figure. The ratio of length of the fundamental unit vector **B** to that of **A** is 1.02, and the angle between **A** and **B** is 59.4°. Consequently, the two-dimensional structure of $(C_2F)_n$ is regarded as a monoclinic system.

ESCA Measurement. ESCA spectra were obtained by a DuPont ESCA 650B electron spectrometer (Shimadzu Seisakusho Ltd.) with an Mg $K\alpha_{1,2}$ X-ray source (1253.6 eV). Binding energies were all measured relative to the C_{1s} peak (285.0 eV) due to hydrocarbon contamination which built up slowly on the surface under these operating conditions.

Figure 12 shows typical spectra of electrons from the 1s orbital of carbon atoms in graphite fluoride. In addition to the main peak at 290.4 eV (A_1), the spectra of samples F and I corresponding to $(CF)_n$ show a broad shoulder centered at 292.4 eV (A_2) and a low-intensity tail centered at about 294 eV (A_3), and these peaks are assigned to >CF, $>CF_2$, and $-CF_3$ carbons, respectively.[15,39,64] However, the spectra of samples G and H corresponding to $(C_2F)_n$ indicate another distinguished shoulder at 288.5 eV (A_4) in addition to the three

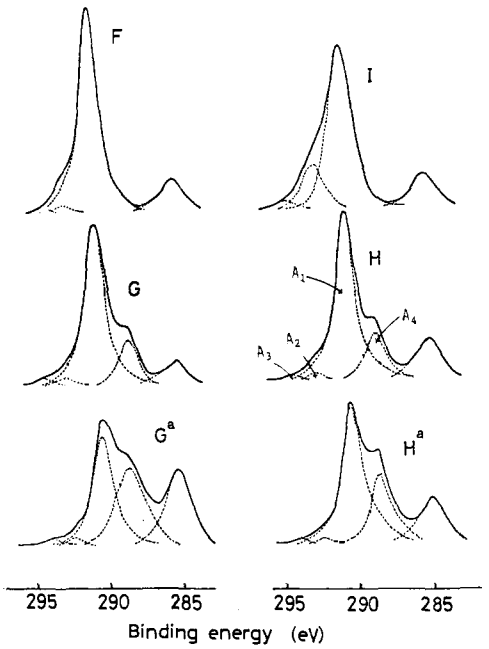

Figure 12. C_{1s} spectra of graphite fluoride.

Table III. Binding Energies for C_{1s} and F_{1s} Levels of Graphite Fluoride

sample	C_{1s} peak, eV				F_{1s} peak, eV
	A_1	A_2	A_3	A_4	A_5
F	290.4	292.4	294.1		689.6
I	290.4	292.4	294.4		689.6
G	290.2	292.4	293.9	288.4	689.3
H	290.4	292.5	294.1	288.5	689.3

peaks described above. The binding energies for the C_{1s} level are summarized in Table III together with those of the F_{1s} level. The binding energies approximately agree with one another.

The spectrum of sample F* obtained by grinding sample F with agate mortar is similar to that of the original sample. For the samples G and H, however, the peak (A_4) of the spectra of ground samples becomes larger in comparison with the original sample.

The probability of primary photoelectron escaping from a depth, x, below the surface of a solid A in an ESCA measurement is proportional to $\exp(-x/\lambda_A)$, where λ_A is the inelastic mean free path for the electron in the solid. Since the X-ray penetration depth is large compared with λ, the total ESCA peak intensity I_A is proportional to $\int_0^\infty \exp(-x/\lambda_A)\,dx$ and is also proportional to the cross section, σ_A, for photoionization in a given shell of a given atom and the number of atoms of A per unit volume, N_A. Hence

$$I_A = k\sigma_A N_A \lambda_A \qquad (1)$$

where k is a constant for given experimental conditions (X-ray flux, sample geometry, etc.).[66] Thus, observation of signal intensities in ESCA spectra can provide semiquantitative analysis of elements on the surface.

The area ratios of the various core photoelectron peaks to the peak A_1 are tabulated in Table IV. The composition of sample I prepared from petroleum coke with small crystallite is $CF_{1.13}$, which possesses a number of $>CF_2$ groups. In the spectra of $(CF)_n$, the intensity ratio of total C_{1s} peaks to F_{1s} peak is about 0.23, which nearly agrees with the value (0.27) reported by Jørgensen and Berthou.[67] On the other hand, in the spectra of $(C_2F)_n$, if it is assumed that the peak A_4 arises from carbon atoms bonded with fluorine, the intensity ratios shown in the seventh column of Table IV become large values in comparison with those of $(CF)_n$, and, if the peak A_4 is assumed to be due to nonbonded carbon atoms with fluorine, the intensity ratio of each sample agrees with that of $(CF)_n$ as shown in the eighth column of the same table. Consequently, $(C_2F)_n$ is expected for the carbons which are not combined with fluorine in addition to $>CF_2$ and $-CF_3$ groups at the edges of the graphite fluoride layers and tertiary $>CF$ as is the case with $(CF)_n$. The intensity ratio of the peak A_4 to A_1 may be regarded as approaching unity by the grinding of the sample. The chemical shift seems to be due to neighboring carbons bonded with fluorine.

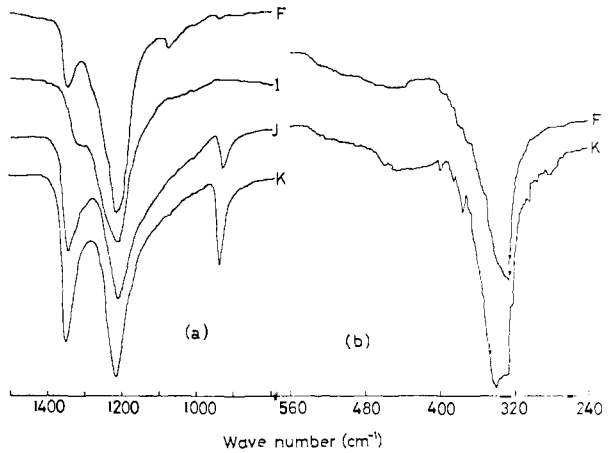

Figure 13. IR spectra of graphite fluoride.

IR Measurement. Infrared spectra (4000–650 cm^{-1}) were taken on a Shimadzu IR-27G spectrometer using KBr disk samples, and far-infrared spectra (650–250 cm^{-1}) were taken on a Hitachi FIS-3 spectrometer using Nujol mull samples.

Figure 13 shows infrared and far-infrared spectra of graphite fluoride. The strongest bands at 1219 cm^{-1} of $(CF)_n$ (sample F) and at 1221 cm^{-1} of $(C_2F)_n$ (samples J and K) are assigned to the C–F stretching vibration of tertiary carbon atoms.[4,9,32] Furthermore, in the spectra of $(CF)_n$, two medium bands at 1350 and 1075 cm^{-1} were observed, and also a very weak band at 940 cm^{-1} was noted. On the other hand, in the spectra of $(C_2F)_n$, the bands at 1354 and 940 cm^{-1} become strong and the band at 1075 cm^{-1} is hardly observed. The bands at 1354 and 1075 cm^{-1} have been regarded as being due to asymmetric and symmetric stretching vibrations, respectively, of the peripheral $>CF_2$ groups,[32] but these bands were not observed in the spectra of sample I, which contains a number of $>CF_2$ groups.

In the far-infrared region where skeletal vibrations are observed, the strong bands at 332 cm^{-1} in the spectra of $(CF)_n$ and 340 cm^{-1} in those of $(C_2F)_n$ were observed. In the spectra of $(C_2F)_n$, many very weak bands were also noted.

NMR Measurement. The ^{19}F resonances were observed in a field of 6230–6260 G at 25 MHz. Figure 14 shows the absorption derivatives for the ^{19}F resonance in graphite fluoride. The values of the second moment may be computed directly from the measured derivative of the absorption line, and comparison with theoretical values obtained from the Van Vleck formula[68] can provide an examination of the validity of any assumed structure. The second moment for powder samples can be calculated from the relation

$$\langle \Delta H_2^2 \rangle = \frac{6}{5}\gamma^2\hbar^2 I(I+1)\frac{1}{N}\sum_{i>j} r_{ij}^{-6} \qquad (2)$$

where r_{ij} is the internuclear distance between dipoles i and j of gyromagnetic ratio γ and spin I, and N is the number of the

Table IV. Area Ratios for C_{1s} and F_{1s} of Graphite Fluoride

sample	C_{1s} peak A_1	A_2	A_3	A_4	F_{1s} peak A_5	$(A_1 + 2A_2 + 3A_3 + A_4)/A_5$	$(A_1 + 2A_2 + 3A_3)/A_5$
F	100	2.5	1.7	0	477.1	0.231	0.231
F[a]	100	2.3	1.1	0	461.4	0.234	0.234
I	100	24.2	4.9	0	742.7	0.220	0.220
G	100	3.1	3.6	26.0	525.3	0.272	0.223
G[a]	100	3.1	3.1	86.6	496.2	0.407	0.233
H	100	1.7	1.4	24.5	463.8	0.285	0.232
H[a]	100	2.1	1.0	48.0	447.4	0.347	0.240

[a] Sample ground with an agate mortar.

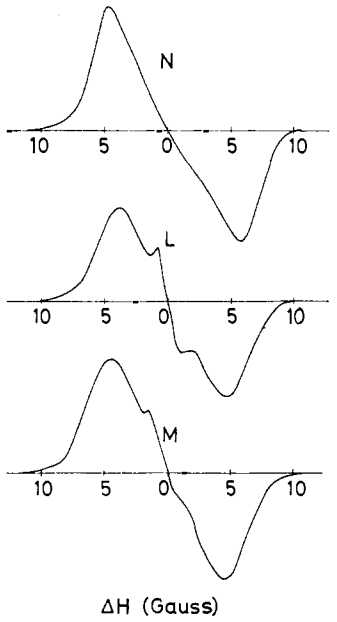

Figure 14. Absorption derivatives for ^{19}F resonance in graphite fluoride.

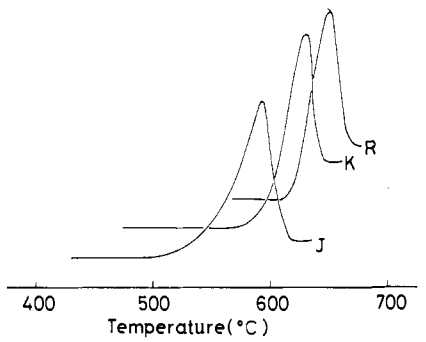

Figure 15. DTA curves of graphite fluoride under an argon atmosphere (heating rate 10 °C/min).

nuclei at resonance which are present in the elementary dipole-interaction cell.

Ebert et al.[37] have proposed the structure of $(CF)_n$ that consists of arrays of cis-trans-linked cyclohexane rings in the boat conformation based on the assumption of a Gaussian line shape model for the absorption line of $(CF_{1.06})_n$ and $(CF_{1.15})_n$. However, the absorption line obtained from sample *N* was not a Gaussian, and the second moment obtained from the absorption line is 10.6 G^2.[69] The theoretical second moments for boat and chair models on the basis of the data of X-ray diffractometry are 21.7 and 9.7 G^2,[37] respectively, and the experimental second moment is consistent with the chair model for $(CF)_n$. Furthermore, the existence of a sixfold rotating axis in the electron diffraction pattern of $(CF)_n$ is in favor of the chair structure because the boat structure of $(CF)_n$ belongs to an orthorhombic system.

Table V. Composition, Surface Area, and Heat of Immersion of Graphite Fluoride

sample	composition	surface area, m^2/g	heat of immersion, $ergs/cm^2$
original graphite		6.0	138[a]
O	$CF_{0.57}$	28.2	55
P	$CF_{0.58}$	117.0	53
Q	$CF_{0.86}$	116.7	45
N	$CF_{1.00}$	126.7	39
PTFE			56[b]

[a] See ref 70. [b] See ref 71.

The absorption lines of $(C_2F)_n$ consist of the broad- and narrow-line components. The narrow-line component does not disappear even in the sample M heat-treated at 600 °C. The second moments obtained from the absorption lines of samples L and M were 10.2 and 9.7 G^2, respectively.

DTA. Figure 15 shows the DTA curves for graphite fluoride. The thermal decomposition of $(C_2F)_n$ prepared at 375 °C occurs at about 490 °C. However, when such low-crystalline $(C_2F)_n$ is heat-treated at 600 °C for 120 h, it leads to the high crystallinity so that the thermal decomposition did not occur up to 570 °C. The thermal stability of $(C_2F)_n$ is somewhat inferior to that of $(CF)_n$.

Heat of Immersion. Samples were degassed at 150 °C for at least 1.5 h under a reduced pressure of about 10^{-3} mmHg and sealed in an ampule. The heat of immersion was measured by using a LKB microcalorimeter 2107 which was placed in a constant-temperature vessel maintained at 25 °C. Reagent grade *n*-butyl alcohol was used as a wetting liquid.

Table V shows the composition, surface area, and heat of immersion of graphite fluoride. The heat of immersion of graphite fluoride increases with decreasing the fluorine content, and that of $(CF_{0.57})_n$ is equal to that of PTFE. The heat of immersion was somewhat affected by the heat-treatment of the sample.

The surface area of graphite fluoride is strongly dependent on the reaction and treatment temperatures, and increases with increasing the temperatures because of the pyrolysis and the exfoliation of the sample.

Crystal Structure of $(C_2F)_n$. From the above results, the layered structure of $(C_2F)_n$ may be considered as shown in Figure 16. The lattice parameters were calculated on the basis of the results of X-ray and electron diffractometries. A rhomb shown by a dashed line is a unit cell, a = 5.01 Å, b = 4.92 Å; the angle between a and b, γ = 120.6°.[72] As the lengths of C—C and C=C bonds are assumed to be 1.54 and 1.33 Å, respectively, the C—C—C bond angles (sp^3 carbons) and C—C=C bond angle (sp^2 carbons) are calculated to be 108.6, 109.9, and 120.8°, respectively. The unit cell consists of eight carbon atoms (0 0 0, 0.003 0.501 $-0.387/c$, 0.157 0.314 0, 0.157 0.813 $0.387/c$, 0.500 0 0, 0.503 0.501 $0.387/c$, 0.657 0.314 0, 0.657 0.813 $-0.387/c$) and four fluorine atoms (0.028

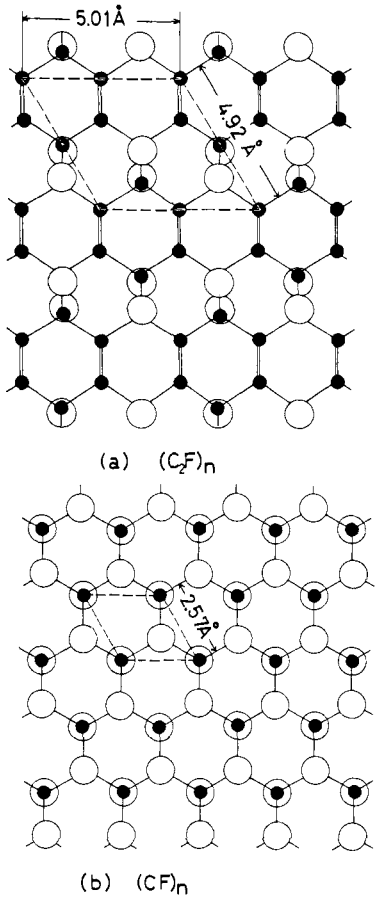

Figure 16. Layered structure of (a) $(C_2F)_n$ and (b) $(CF)_n$: ●, carbon; ○, fluorine.

0.556 $-1.78/c$, 0.129 0.759 $1.78/c$, 0.528 0.556 $1.78/c$, 0.629 0.759 $-1.78/c$)[73] where c is the lattice constant of the c axis.

According to these values, each interplanar spacing of $(C_2F)_n$ is given by the equation

$$\frac{1}{d^2_{(hkl)}} = \frac{1}{\sin^2\gamma}\left(\frac{h^2}{a^2} + \frac{k^2}{b^2} - \frac{2hk\cos\gamma}{ab} + \frac{l^2\sin^2\gamma}{c^2}\right) \quad (3)$$

where $d_{(hkl)}$ is the interplanar spacing of (hkl) plane. The index l should be zero when a two-dimensional plane is considered. The diffraction lines having a peak at 40.85 and 74.7° in Figure 9 are assigned to (200) and (220), respectively.

The three-dimensional structure of $(C_2F)_n$ may be composed of random stacking because (hkl) reflections are missing in the diffraction pattern. The interlayer spacing of $(C_2F)_n$ is very larger than that of $(CF)_n$. This reason is not obvious but the fluorine absorbed into the interlayer of $(C_2F)_n$ might be responsible for the large interlayer spacing. Even in $(C_4F)_n$, the hydrogen fluoride absorbed into the interlayer of the sample could not be completely removed in a warm vacuum environment.

In conclusion, the structure of $(C_2F)_n$ is considered to consist of layers (Figure 16) stacked parallel at the same distance of about 8.8 Å, but with each layer having a completely random orientation.

III. Formation Process of $(C_2F)_n$ and $(CF)_n$. It was revealed that a mixture of $(C_2F)_n$ and $(CF)_n$ was produced by the fluorination of graphite at temperatures below 600 °C. There is no definite boundary between the formation temperatures of both compounds.

In this section, by using flaky graphite as the starting material, a study is made on the formation process of $(C_2F)_n$ and

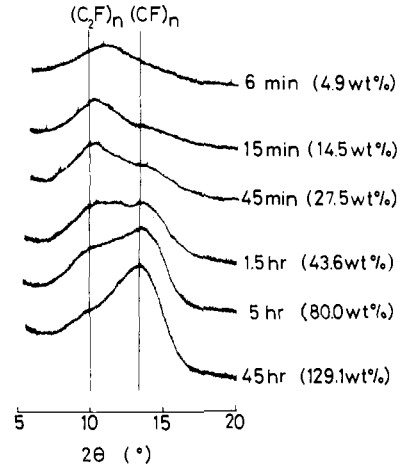

Figure 17. Variation of (001) diffraction partern of graphite fluoride prepared with reaction time at 485 °C.

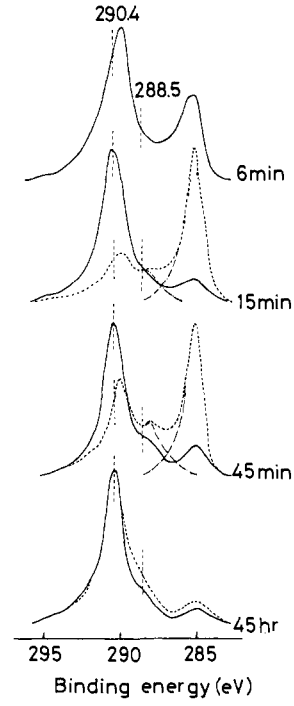

Figure 18. Variation of C_{1s} spectra with reaction time: dashed line, ground sample.

$(CF)_n$ under fixed reaction conditions by means of thermogravimetry, X-ray diffractometry, and ESCA.

Figure 17 shows the variation of the (001) diffraction pattern of graphite fluoride with the reaction time of the fluorination of graphite at 485 °C. The weight increase[74] due to the fluorination is shown with the number in parentheses. In the initial stage of reaction, the diffraction line due to $(C_2F)_n$ (2θ = 10.3°) appears, but that due to $(CF)_n$ (2θ = 13.6°) strongly emerges with the progress in fluorination. The ratio of the intensity at 13.6° to that at 10.3° tends to increase when the weight increase exceeds about 20 wt %. This indicates that the fluorination first leads to the formation of $(C_2F)_n$, but further fluorination leads subsequently to the formation of $(CF)_n$. The product completely fluorinated at 485 °C is $CF_{0.81}$, that is, a mixture of $(C_2F)_n$ and $(CF)_n$ with a ratio 38:62. Supposing that $(C_2F)_n$ is first formed, the weight increase at the transition from the formation of $(C_2F)_n$ to that of $(CF)_n$ is in fair agreement with that obtained from Figure 17.

A further analysis of the formation process of graphite fluoride was carried out by ESCA. Figure 18 shows the C_{1s}

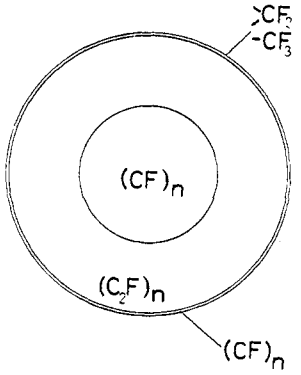

Figure 19. Schematic illustration of composition of nonstoichiometric graphite fluoride.

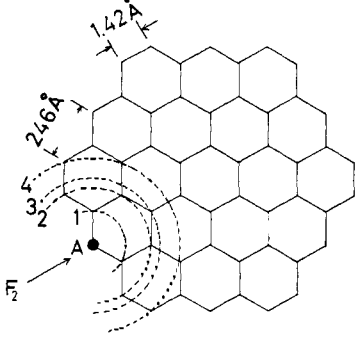

Figure 20. Schematic illustration of fluorination process of graphite.

spectra of products prepared at 485 °C for various reaction times. The dashed curves represent C_{1s} spectra of the samples ground in an agate mortar. As far as the intensity ratio of the peak at binding energy 288.5 eV arising from $(C_2F)_n$ to the peak at 290.4 eV assigned to the tertiary >CF carbons of $(C_2F)_n$ and $(CF)_n$ in products prepared for 15 and 45 min,[75] the ratio is small compared with that of each ground sample. This indicates that the extremely thin film of graphite surface is fluorinated to $(CF)_n$. The thickness of this film is presumed to be less than 100–1000 Å from the measurements by X-ray diffractometry and ESCA. Based on these results, it is possible to interpret that graphite fluoride prepared from petroleum coke[14] and carbon black[24] with the small crystallite consists of almost $(CF)_n$ even at low reaction temperatures of 300–400 °C.

Consequently, the fluorination of graphite first leads to the formation of $(CF)_n$ in the thin film of surface which is easily fluorinated, followed by the formation of $(C_2F)_n$, and further fluorination again leads to the formation of $(CF)_n$. Since the fluorination of graphite occurs along a direction parallel to the basal plane of graphite crystal, the composition of graphite fluoride prepared by the fluorination of disk-like graphite particles in the temperature range of 400–600 °C is schematically shown in Figure 19. There are $>CF_2$ and $-CF_3$ groups around the edges of the layers, and the $(C_2F)_n$ content depends on the carbon materials and the reaction conditions. However, it is inadequate to assume that the sample is the disk-type particle because of the crystal defects of the original graphite and the cracks of the sample resulting from the fluorination,[15] and in practice, it should be considered as an assembly of these crystallites.

Let us discuss the mechanism of the formation process of $(C_2F)_n$ and $(CF)_n$. Figure 20 shows the layered structure of graphite. Suppose that the fluorination proceeds from the direction as shown in the figure. If fluorine first combines with carbon at the site A, then the subsequent sites of carbon to be combined with fluorine are as follows:[76] (1) a first-neighbor carbon (interatomic distance of C–C, 1.42 Å); (2) a second-neighbor carbon (interatomic distance of C–C, 2.46 Å); (3) a third-neighbor carbon (interatomic distance of C–C, 2.84 Å); (4) a fourth-neighbor carbon (interatomic distance of C–C, 3.76 Å). The position of each kind of neighboring carbons is connected by the chain circles 1–4 which have a common center at A. The cases of (1), (2), or (3) correspond to the formation of $(CF)_n$ composed of cyclohexane rings in a boat conformation,[65] of $(CF)_n$ composed of cyclohexane rings in a chair conformation, or of $(C_2F)_n$, respectively. If fluorine combines with the sixth-neighbor carbons (interatomic distance of C–C, 4.92 Å), $(C_4F)_n$ is formed.

At first $(CF)_n$ is formed on an easily fluorinated surface, and then fluorine combines with the third-neighbor carbon so that $(C_2F)_n$ is formed. When combined covalently with fluorine, carbon atoms lead to sp^3 hybridization. Accordingly, an internal stress is built up in both fluorinated and unreacted graphites because of the expansion of the carbon hexagon network. Especially, the lattices in the vicinity of the reaction interface are subject locally to a large stress, and C–F bonds are also not completely covalent bonds. These strains and the rate of transition of weak carbon–fluorine bond to covalent bond increase with the progress of the fluorination because of the presence of fluorinated graphite. Thus the variation of the lattice strain and the character of bonding between fluorine and carbon with the progress of the reaction bring about a change in the geometry of the potential energy surface. Consequently, fluorine combines with the second-neighbor carbon so that $(CF)_n$ is formed.

Based on the above presumption, it is possible to interpret all the experimental results. As the crystallization rate of the fluorinated graphite increases with the elevation of reaction temperature, the strain of unreacted graphite will also increase. Therefore, fluorine is liable to combine with the second-neighbor carbons and the $(CF)_n$ content increases. On the other hand, at a fixed temperature, as the reaction rate increases with increasing fluorine pressure, higher fluorine pressure leads to a slowdown of the crystallization of fluorinated graphite near the reaction interface. Therefore, the strain of unreacted graphite is small so that the $(CF)_n$ content decreases. As the crystallization rate of graphite fluoride is strongly dependent on the reaction temperature and the crystallite size of carbon materials, it is also understandable that the composition is strongly dependent on these factors.

Conclusion

The formation of a novel chemical compound, "polydicarbon monofluoride", represented by the formula $(C_2F)_n$, was confirmed under relatively mild reaction conditions. The composition of graphite fluoride with F/C ratio less than unity varies no longer even after the treatment at higher temperature in a fluorine atmosphere. However, its color varied from black to white. Accordingly, the color of graphite fluoride does not depend on the composition but on the reaction and treatment temperatures.

The structure of $(CF)_n$ consists of layers (lattice constant $a = b = 2.57$ Å) with trans-linked cyclohexane rings in the chair conformation stacked randomly at the same distance of about 5.9 Å.

The arrangement of two-dimensional lattice points of $(C_2F)_n$ shows a twofold rotating symmetry, and the two-dimensional structure is regarded as a monoclinic system. The lattice constants are $a = 5.01$ Å, $b = 4.92$ Å, and $\gamma = 120.6°$. The lengths of C—C, C=C, and C—F bonds are 1.54, 1.33, and 1.41 Å, respectively. The C—C—C bond angles (sp^3 carbons) and C—C=C bond angle (sp^2 carbons) are 108.6, 109.9, and 120.8°, respectively. The unit cell consists of eight carbon atoms and four fluorine atoms. The stacking of the above layers is a turbostratic structure which consists of layers stacked

randomly at the same distance of about 8.8 Å. The thermal stability of $(C_2F)_n$ is improved by the heat-treatment under fluorine atmosphere, and is somewhat inferior to that of $(CF)_n$. The heat of immersion of graphite fluoride increases with decreasing the fluorine content, and that of $(C_2F)_n$ is equal to that of PTFE.

When graphite is fluorinated at temperatures below 600 °C, at first $(CF)_n$ is formed as an extremely thin film on graphite surface, and then fluorine combines with the third-neighbor carbons so that $(C_2F)_n$ is formed. As the fluorination further proceeds, fluorine combines with the second-neighbor carbons so that $(CF)_n$ is again formed. This is due to the variation of the lattice strain of the unreacted carbon hexagon network and the character of bonding between fluorine and carbon in the vicinity of the reaction interface with the progress of fluorination.

Acknowledgment. The authors would like to thank the Laboratory for Organic Elemental Microanalysis, Faculty of Pharmaceutical Sciences, Kyoto University, for the elemental analyses, Dr. H. Takenaka of Government Industrial Research Institute, Osaka, for the measurement of the heat immersion, and Dr. F. Nakamura, Kyoto University for NMR studies

References and Notes

(1) O. Ruff and O. Bretschneider, *Z. Anorg. Allg. Chem.*, **217**, 1 (1937).
(2) W. Rüdorff and G. Rüdorff, *Z. Anorg. Allg. Chem.*, **253**, 281 (1947).
(3) W. Rüdorff and G. Rüdorff, *Chem. Ber.*, **80**, 413 (1947).
(4) W. Rüdorff and K. Brodersen, *Z. Naturforsch. B*, **12**, 595 (1957).
(5) W. Rüdorff, *Adv. Inorg. Chem. Radiochem.*, **1**, 230 (1959).
(6) N. Watanabe and M. Ishii, *Denki Kagaku*, **29**, 364 (1961).
(7) N. Watanabe, M. Inoue, and S. Yoshizawa, *Denki Kagaku*, **31**, 693 (1963).
(8) N. Watanabe and M. Nishimura, *Yōyūen*, **11**, 267 (1968).
(9) N. Watanabe, Y. Koyama and S. Yoshizawa, *Denki Kagaku*, **31**, 756 (1963).
(10) N. Watanabe and K. Kumon, *Denki Kagaku*, **35**, 19 (1967).
(11) N. Watanabe and A. Shibuya, *Kogyo Kagaku Zasshi*, **71**, 968 (1968).
(12) N. Watanabe and M. Takashima, *Kogyo Kagaku Zasshi*, **74**, 1788 (1971).
(13) N. Watanabe, H. Takenaka and M. Takashima, *Nippon Kagaku Kaishi*, 487 (1973).
(14) N. Watanabe, M. Takashima, and K. Takahashi, *Nippon Kagaku Kaishi*, 1033 (1974).
(15) N. Watanabe and H. Takenaka, 5th European Symposium on Fluorine Chemistry, Aviemore, Scotland, Sept. 16–20, 1974.
(16) M. Takashima and N. Watanabe, *Nippon Kagaku Kaishi*, 432 (1975).
(17) N. Watanabe, H. Takenama, and S. Kimura, *Nippon Kagaku Kaishi*, 1655 (1975).
(18) N. Watanabe and Y. Kita, *Nippon Kagaku Kaishi*, 1896 (1975).
(19) H. Imoto, T. Nakajima, and N. Watanabe, *Bull. Chem. Soc. Jpn.*, **48**, 1633 (1975).
(20) H. Imoto and N. Watanabe, *Bull. Chem. Soc. Jpn.*, **49**, 1736 (1976).
(21) M. Takashima and N. Watanabe, *Nippon Kagaku Kaishi*, 1222 (1976).
(22) N. Watanabe and Y. Kita, *Tanso*, **84**, 2 (1976).
(23) N. Watanabe, Y. Kita, and T. Kawaguchi, *Nippon Kagaku Kaishi*, 191 (1977).
(24) N. Watanabe, Y. Kita, and O. Mochizuki, IUPAC Congress, Tokyo, Japan, Sept 4–10, 1977.
(25) A. K. Kuriakose and J. L. Margrave, *J. Phys. Chem.*, **69**, 2772 (1965).
(26) A. K. Kuriakose and J. L. Margrave, *Inorg. Chem.*, **4**, 1639 (1965).
(27) J. L. Wood, R. B. Badachhape, R. J. Lagow, and J. L. Margrave, *J. Phys. Chem.*, **73**, 3139 (1969).
(28) R. J. Lagow, R. B. Badachhape, P. Ficalora, J. L. Wood, and J. L. Margrave, *Synth. Inorg. Met.-Org. Chem.*, **2**, 145 (1972).
(29) J. L. Wood, A. J. Valerga, R. B. Badachhape, and J. L. Margrave, Final Report, Contract DAAB07-72-C-0105 (ECOM), Rice University, Nov 1973.
(30) A. J. Valerga, R. B. Badachhape, G. D. Parks, P. Kamarchik, J. L. Wood, and J. L. Margrave, Final Report, Contract DAAB07-73-C-0056 (ECOM), March 1974.
(31) R. J. Lagow, R. B. Badachhape, J. L. Wood, and J. L. Margrave, *J. Am. Chem. Soc.*, **96**, 2628 (1974).
(32) R. J. Lagow, R. B. Badachhape, J. L. Wood, and J. L. Margrave, *J. Chem. Soc., Dalton, Trans.*, 1268 (1974).
(33) V. K. Mahajan, R. B. Badachhape, and J. L. Margrave, *Inorg. Nucl. Chem. Lett.*, **10**, 1103 (1974).
(34) D. E. Palin and K. D. Wadsworth, *Nature (London)*, **162**, 925 (1948).
(35) M. L. Bernard, A. Hardy, P. Hobbes, R. Lucas, and M. Roux, *Bull. Soc. Chim. Fr.*, 2129 (1972).
(36) D. E. Parry, J. M. Thomas, B. Bach, and E. L. Evans, *Chem. Phys. Lett.*, **29**, 128 (1974).
(37) L. B. Ebert, J. I. Brauman, and R. A. Huggins, *J. Am. Chem. Soc.*, **96**, 7841 (1974).
(38) D. T. Clark and J. Peeling, *J. Polym. Sci., Polym. Chem. Ed.*, **14**, 2941 (1976).
(39) P. Cadman, J. D. Scott, and J. M. Thomas, *Carbon*, **15**, 75 (1977).
(40) T. Ishikawa and T. Shimada, 5th International Fluorine Symposium, Moscow, 1969.
(41) R. L. Fusaro and H. E. Sliney, *ASLE Trans.*, **13**, 56 (1970).
(42) H. Gisser, M. Petronio, and A. Shapiro, *Lubr. Eng.*, **28**, 161 (1972).
(43) R. L. Fusaro and H. E. Sliney, *ASLE Trans.*, **16**, 189 (1973).
(44) Y. Tsuya, H. Uemura, Y. Okamoto, and S. Kurosaki, ASLE/ASME Lubrication Conference, Atlanta, 1973.
(45) C. Martin, J. Sullean, and M. Roussel, *Wear*, **34**, 215 (1975).
(46) N. Watanabe and M. Fukuda, U.S. Patent 3 536 532 (Oct 27, 1970).
(47) H. F. Hunger and G. J. Heymach, *J. Electrochem. Soc.*, **120**, 1161 (1973).
(48) J. J. Auborn, K. W. French, S. I. Lieberman, V. K. Shah, and A. Heller, *J. Electrochem. Soc.*, **120**, 1613 (1973).
(49) W. K. Behl, J. A. Christopulos, M. Ramirez, and S. Gilman, *J. Electrochem. Soc.*, **120**, 1619 (1973).
(50) W. Tiedemann, *J. Electrochem. Soc.*, **121**, 1308 (1974).
(51) M. S. Whittingham, *J. Electrochem. Soc.*, **122**, 526 (1975).
(52) H. F. Hunger and J. E. Ellison, *J. Electrochem. Soc.*, **122**, 1288 (1975).
(53) In the present study, the samples with particle size of 20–50 and 200–250 mesh are designated as flaky sample and powder sample, respectively.
(54) K. Hozumi and N. Akimoto, *Jpn. Anal.*, **20**, 467 (1971).
(55) W. Schöniger, *Mikrochim. Acta*, 123 (1955); 869 (1956).
(56) The formation time is defined as the time required to completely fluorinate graphite.
(57) Rapid heating leads to the decomposition of the product because of the heat of crystallization and the slow rate of crystallization of graphite fluoride.
(58) As the (001) diffraction lines of the products obtained between 450 and 525 °C are extremely broad, errors in the values of $d_{(001)}$ and $\beta_{(001)}$ seem to be unavoidable.
(59) This is because the product from flaky graphite has a little background scattering.
(60) N. Watanabe and H. Takenaka, *Netsusokutei*, **3**, 105 (1976).
(61) According to Warren,[62,63] the peak of a two-dimensional lattice reflection (*hk*) in a random layer lattice is displaced toward a larger angle from the position of the corresponding crystalline reflection (*hk*0) by an amount of $\Delta(\sin\theta) = 0.16\lambda/L_a$, where λ is the wavelength of the X-ray and L_a is the crystallite diameter. Taking into account this consideration, the lattice constant of $(CF)_n$ becomes 2.59 Å.
(62) B. E. Warren, *Phys. Rev.*, **59**, 693 (1941).
(63) J. Biscoe and B. E. Warren, *J. Appl. Phys.*, **13**, 364 (1942).
(64) P. Cadman, J. D. Scott, and J. M. Thomas, *J. Chem. Soc., Chem. Commun.*, 654 (1975).
(65) In the lower layer, fluorine combines with the third-neighbor carbon.
(66) P. Cadman, S. Evans, J. D. Scott, and J. M. Thomas, *J. Chem. Soc., Faraday Trans. 2*, 1777 (1975).
(67) C. K. Jørgensen and H. Berthou, *Faraday Discuss. Chem. Soc.*, **54**, 269 (1972).
(68) J. H. Van Vleck, *Phys. Rev.*, **74**, 1168 (1948).
(69) Assuming a Gaussian line shape model, the second moment is 24.5 G^2.
(70) S. S. Barton, G. L. Boulton, and B. H. Harrison, *Carbon*, **10**, 391 (1972).
(71) R. J. Good, L. A. Girifalco, and G. Kraus, *J. Phys. Chem.*, **62**, 1418 (1958).
(72) This is not a conventional way of selecting crystallographic axes, but is employed in order to easily compare with that of $(CF)_n$.
(73) The bond length of C–F is assumed to be 1.41 Å.
(74) The weight increase, *W*, is defined as follows: *W* = (wt of fluorinated graphite − original wt of graphite)/original wt of graphite. Therefore, if graphite is completely changed into $(CF)_n$, its weight increase is theoretically (19.00/12.00) × 100 = 158.3 wt %.
(75) The binding energy of these peaks is lower than those of the crystalline graphite fluoride, because these products must be very strained and the C–F bond is not a completely covalent bond.[15]
(76) In the following discussion, only the fluorine in the upper layer of graphite is considered.